MAGNETICS®

Division of Spang & Company

Inverter Transformer Core Design and Material Selection

TABLES

FIGURES

ACKNOWLEDGEMENT

This paper has been prepared by, and is used with the permission of

Colonel Wm. T. McLyman, Member of the Technical Staff
Spacecraft Power Section, Guidance and Control Division
Jet Propulsion Laboratory

A Division of Spang & Company

Preface

A program was conducted to study magnetic materials for use in spacecraft transformers used in static inverters, converters, and transformer rectifier supplies. Not only did this program investigate different magnetic alloys best suited for high frequency and high efficiency applications but investigated inherent characteristics of the magnetic materials. One of the characteristics that is detrimental in transformer design is the residual flux density which could be additive on turn-on causing the transformer to saturate. Investigation of this problem led to the design of a transformer with a very low residual flux. When the data of many transformers and in many configurations were compiled the optimum transformer was the transformer with the lowest residual flux that contained a small amount of air gap in the magnetic material.

This program also included a series of tests on magnetic alloys and evaluation of spacecraft transformer design.

The materials evaluated were:

TRADE NAME	MAGNETIC ALLOYS
Orthonol	50% nickel 50% iron
Sq. Permalloy	79% nickel 17% iron 4% moly
48 Alloy	40% nickel 52% iron
Supermalloy	78% nickel 17% iron 5% moly
Magnesil	3% silicon 97% iron

Tests were performed to determine the dc and ac magnetic properties at 2400 Hz using square-wave excitation. These tests were performed on uncut cores which were then cut for comparison of the gapped and ungapped magnetic properties. The data obtained from these tests are described, and the potential uses for the materials are discussed.

Introduction

Static inverters, converters and T-R supplies intended for spacecraft power use are usually of square loop toroidal design. The design of reliable, efficent and lightweight devices of this class for such use has been seriously hampered by the lack of engineering data describing the behavior of both the commonly used and the more exotic core materials with higher frequency square wave excitation.

A program has been carried out at JPL to supply this lack. An investigation has been made to ascertain the dynamic B-H loop characteristics of different core materials presently available from various industry sources. Cores were procured in both toroidal and "C" forms and were tested in both ungapped (uncut) and gapped (cut) configurations. The following describes the results of this investigation.

Typical Operation

Transformers used for inverters, converters and T-R supplies operate from the spacecraft power bus which could be dc or ac. In some power applications, a commonly used circuit is a driven transistor switch arrangement such as that shown in Figure 1.

Figure 1
Typical Driven Transistor Inverter

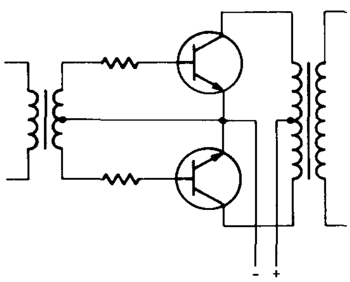

One important consideration affecting the design of suitable transformers is that care must be taken to ensure that operation involves balanced drive to the transformer primary. In the absence of balanced drive, a net dc current will flow in the transformer primary, which causes the core to saturate easily during alternate half-cycles. A saturated core cannot support the applied voltage, and because of lowered transformer impedance the current flowing in a switching transistor is limited only by its beta. Transformer leakage inductance results in a high voltage spike during the switching sequence which could be destructive to the transistors. In order to provide balanced drive, it is necessary to exactly match the transistors for V_{CE}(SAT) and beta and this is not always sufficiently effective. Also exact matching of the transistors is a major problem in the practical sense.

Material Characteristics

Many available core materials approximate the ideal square-loop characteristic illustrated by the B-H curve shown in Figure 2.

Figure 2
Ideal Square B-H Loop

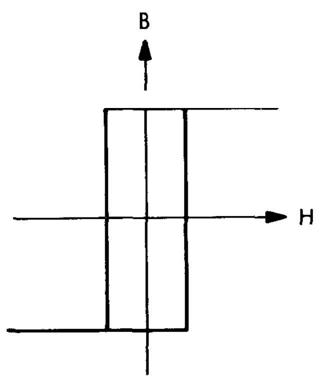

MAGNETICS®
A Division of Spang & Company

Table 1 — Magnetic Core Material Characteristics

TRADE NAMES	COMPOSITION	SATURATED FLUX DENSITY (KG)	DC COERCIVE FORCE (Oe)	SQUARENESS RATIO	MATERIAL DENSITY lb/in³	LOSS FACTOR W/LB AT 3 KHz 5 KG	SPECIFIC GRAVITY
Magnesil Silectron Microsil Supersil	3% Si 97% Iron	15-18	4 - .6	0.85 - 1.0	.276	15.0	7.64
Deltamax Orthonol 49 Square Mu	50% Ni 50% Iron	14 - 16	.1 - .2	0.94 - 1.0	.298	8.00	8.25
Allegheny 4750 48 Alloy Carpenter 49	48% Ni 52% Iron	11.5 - 14	.05 - .15	0.80 - 0.92	.296	5.00	8.20
4-79 Permalloy Sq. Permalloy 80 Sq. Mu 79	79% Ni 17% Iron 4% Moly	6.6 - 8.2	.02 - .04	0.80 - .90	.3156	2.50	8.74
Supermalloy	78% N 17% Iron 5% Moly	6.5 - 8.2	.003 - .008	0.40 - 0.70	.3166	1.70	8.77

Representative dc B-H loops for commonly available core materials are shown in Figure 3. Other characteristics are tabulated in Table 1.

Figure 3
The Typical dc B-H Loops of Magnetic Materials

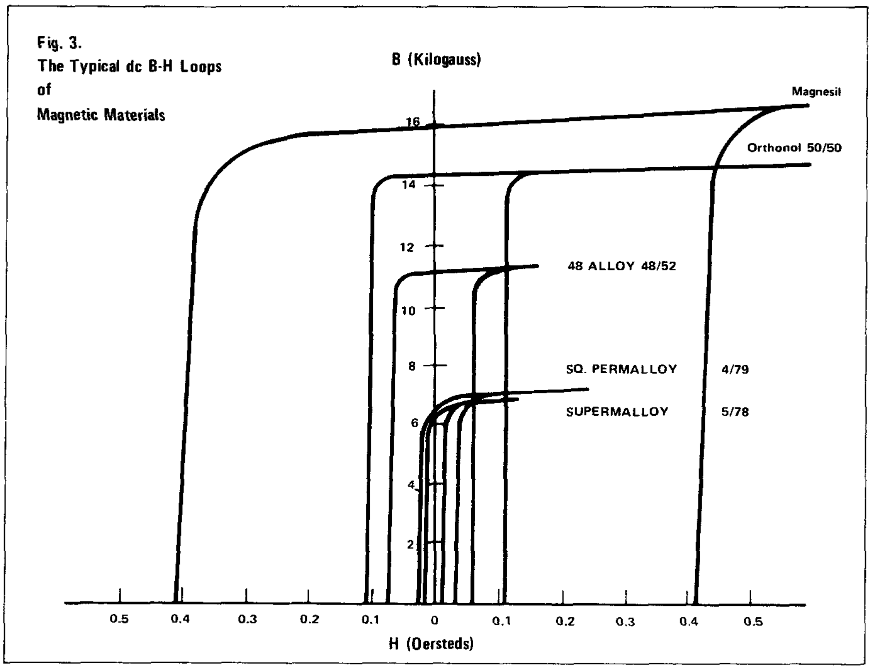

Many articles have been written about inverter and converter transformer design. Usually, the author's recommendation represents a compromise between material characteristics such as those tabulated in Table 1 and the B-H characteristics displayed in Figure 2. These data are typical of commercially available core materials which are suitable for the particular application.

As can be seen, the material which provides the highest flux density (silicon) would result in smallest component size, and this would influence the choice if size is the most important consideration. The type 78 material (see the 78% curve in Figure 3) has the lowest flux density. This results in the largest size transformer, but on the other hand, this material has the lowest coercive force and the lowest core loss of any other core material available.

Usually, inverter transformer design is aimed at the smallest size, with the highest efficiency, and adequate performance under the widest range of environmental conditions. Unfortunately, the core material which can produce the smallest size, has the lowest efficiency. The highest efficiency materials result in the largest size. Thus the transformer designer therefore must make tradeoffs between allowable transformer size and the minimum efficiency which can be tolerated. The choice of core material will then be based upon achieving the best characteristic on the most critical or important design parameter, and acceptable compromises on the other parameters.

Based upon analysis of past design performance, most engineers select size over efficiency as the most important criteria and select an intermediate core material for their designs. Consequently square-loop 50-50 nickel iron has become the most popular material.

Core Saturation Definition

To standardize the definition of saturation, we first define several unique points on the B-H loop as shown in Figure 4.

The straight line through $(H_0, 0)$ and $H_S, B_S)$ may be written as:

$$B = \left(\frac{dB}{dH}\right)(H - H_0) \qquad (1)$$

The line through $(0, B_S)$ and (H_S, B_S) has essentially zero slope and may be written as:

$$B = B_2 \approx B_S \qquad (2)$$

Figure 4

Defining the B-H Loop

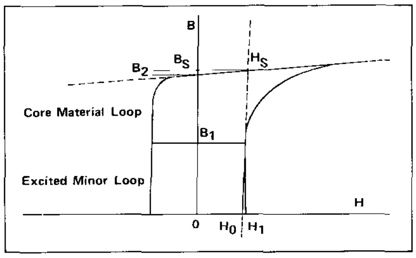

Expressions (1) and (2) together define "saturation" conditions as follows:

$$B_S = \left(\frac{dB}{dH}\right)(H_S - H_0) \qquad (3)$$

Solving (3) for H_S we obtain:

$$H_S = H_0 + \frac{B_S}{\mu_0} \qquad (4)$$

where

$$\mu_0 = \frac{dB}{dH} \text{ by definition}$$

Saturation occurs when the peak exciting current is twice the average exciting current, as shown in Figure 5. Analytically this means that:

$$H_{pk} = 2H_S \qquad (5)$$

Solving (1) for H_1, we obtain:

$$H_1 = H_0 + \frac{B_1}{\mu_0} \qquad (6)$$

To obtain the pre-saturation dc margin (ΔH), we subtract (4) from (3) and obtain:

$$\Delta H = H_S - H_1 = \frac{B_S - B_1}{\mu_0} \qquad (7)$$

The actual unbalanced dc current must be limited to:

N = TURNS

l = mean magnetic length

$$I_{DC} \le \frac{\Delta H\, l}{N} \text{ amperes}$$

Figure 5

Excitation Current

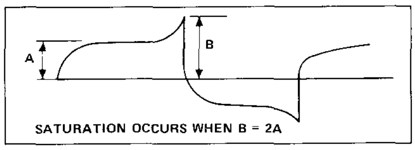

Combining (7) and (8) gives:

$$I_{DC} \le \frac{(B_S - B_1)\ell}{\mu_0 N}, \text{ amperes} \qquad (9)$$

As mentioned earlier, in an effort to prevent core saturation, the switching transistors are matched for beta and V_{CE} (SAT) characteristics. The effect of core saturation using an uncut or ungapped core is shown in Figure 6 which illustrates the effect on the B-H loop when traversed with a dc bias. Figure 6A is a typical B-H loop of 50-50 nickel iron excited from an ac source where the vertical scale is 4 KG/cm.

It can be noted that the minor loop remains at one extreme position within the B-H major loop after removal of dc offset. The unfortunate effect of this random minor loop positioning is that when conduction again begins in the transformer winding, flux swing could begin from the extreme, and not from the normal zero axis. The effect of this is to drive the core into saturation with the production of spikes which can destroy transistors.

The Test Set-Up

A test fixture, schematically indicated in Figure 7, was built to effect comparison of dynamic B-H loop characteristics of various core materials.

Cores were fabricated from various core materials in the basic core configuration designated No. 52029 for toroidal cores manufactured by Magnetics. The materials used were those most likely to be of interest to designers of inverter or converter transformers. Test conditions are listed in Table 2 (page 6).

Winding data was derived from the following:

$$N_T = \frac{V \cdot 10^8}{4.0 \cdot B_m \cdot F \cdot A_c}$$

where

N_T = Number of turns

B_m = Flux density gausses

F = Frequency Hertz

A_c = Core area cm^2

V = Voltage

Figure 6

B-H Loop With dc Bias

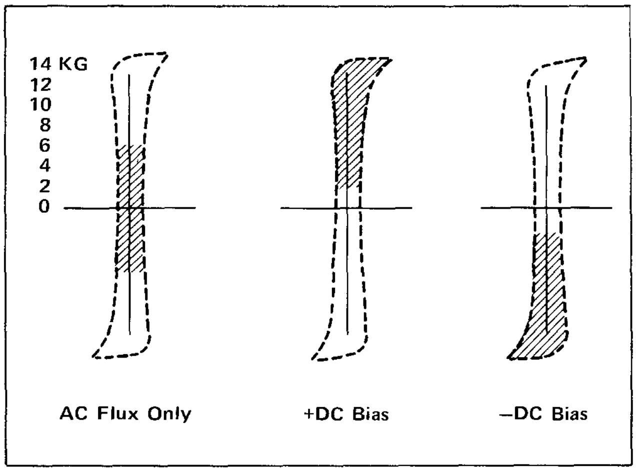

Figure 6A

Typical Square Loop Material With ac Excitation

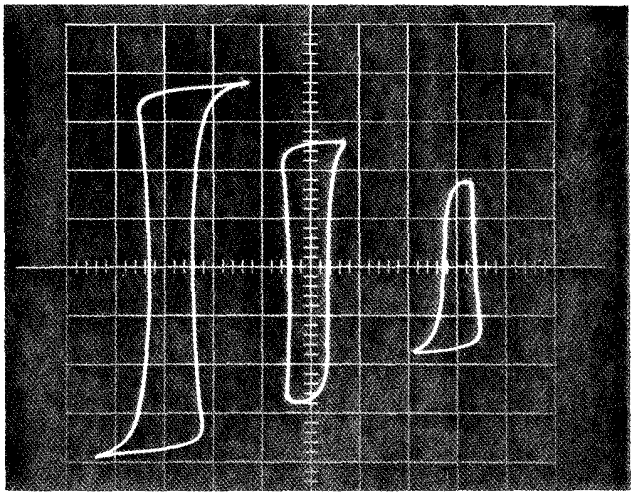

Figure 7

Dynamic B-H Loop Test Fixture

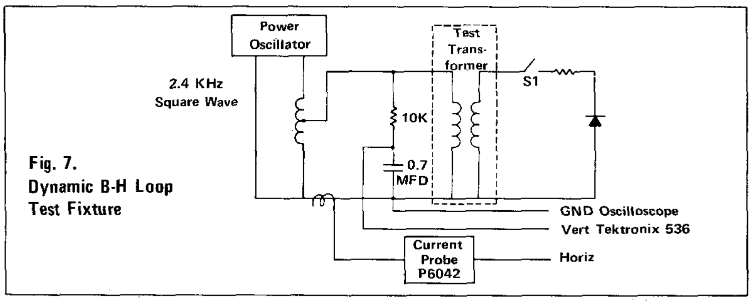

Table 2 — Materials and Constraints

CORE TYPE	MATERIAL	B_m	N_T	FREQ	ml
52029-2A	Orthonol (A)	14.5 KG	54	2.4 KHz	9.47 cm
52029-2D	Sq. Permalloy (D)	7.5 KG	54	2.4 KHz	9.47 cm
52029-2F	Supermalloy (F)	7.5 KG	54	2.4 KHz	9.47 cm
52029-2H	48-Alloy (H)	11.5 KG	54	2.4 KHz	9.47 cm
52029-2K	Magnesil (K)	16.0 KG	54	2.4 KHz	9.47 cm

The test transformer represented in Figure 8 consists of a 54 turn primary and secondary winding, with square wave excitation on the primary. Normally switch S1 is open. With switch S1 closed, the secondary current is rectified by the diode to produce a dc bias in the secondary winding.

Cores were fabricated from each of the materials by winding ribbon of the same thickness on a mandrel of a given diameter. Ribbon termination was effected by welding in the conventional manner.

The photographs designated 9, 10, 11,12 and 13 show the dynamic B-H loops obtained for the different core materials designated therein. Figure 14 shows a composite of all the B-H loops. In each of these, switch S1 was in the open position so that there was no dc bias applied to the core and windings.

The photographs designated Figures 15, 16, 17, 18 and 19 show the dynamic B-H loop patterns obtained for the designated core materials when the test conditions included a sequence in which switch S1 was closed and then opened. It is apparent from these views that with a small amount of dc bias, the minor dynamic B-H loop can traverse the major B-H loop from saturation to saturation. In Figures 15 to 17, it will be noted that after the dc bias had been removed, the minor B-H loops remained shifted to one side or the other. Because of ac coupling of the current to the oscilloscope, the photographs do not present a complete picture of what really happens during the flux swing.

Figure 8
Implementing dc Unbalance

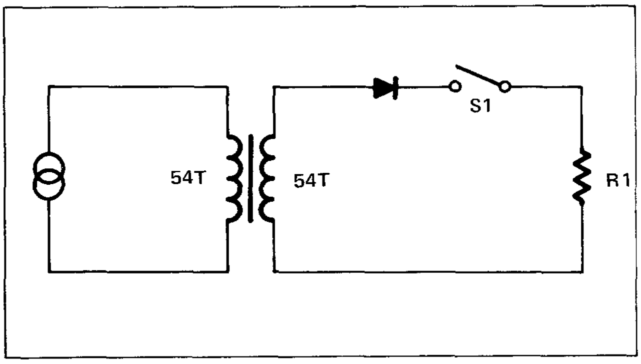

Figure 9

Magnesil K B-H Loop

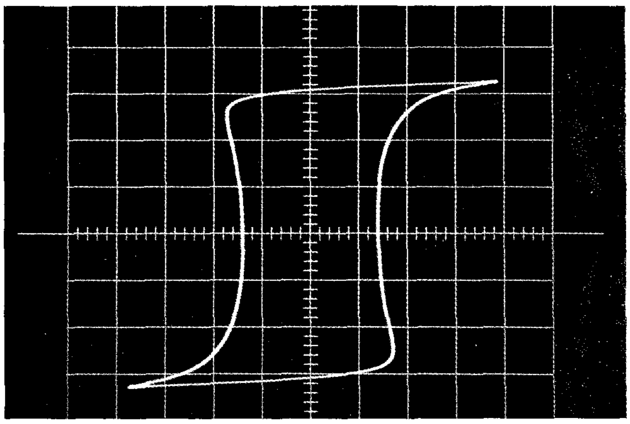

Vert = 5 KG/cm

Horiz = 100 ma/cm

Figure 10

Orthonol A B-H Loop

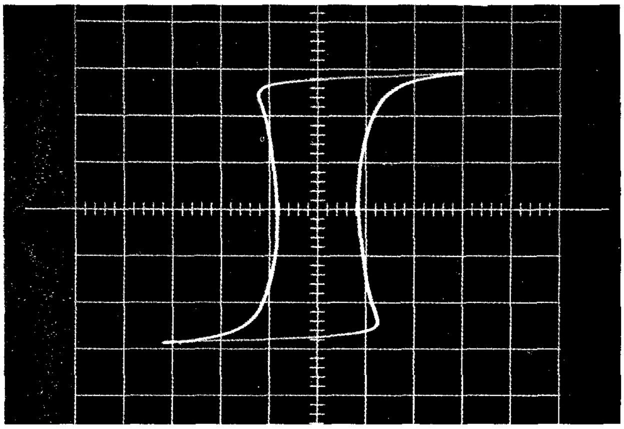

Vert = 5 KG/cm

Horiz = 50 ma/cm

Figure 11

48 Alloy H B-H Loop

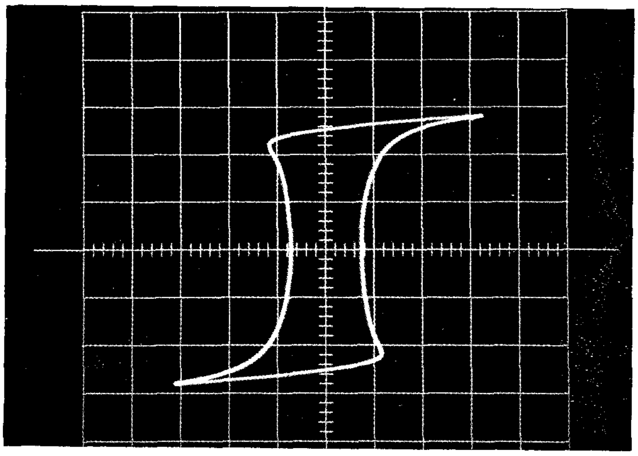

Vert = 5 KG/cm

Horiz = 50 ma/cm

Figure 12

Sq. Permalloy D B-H Loop

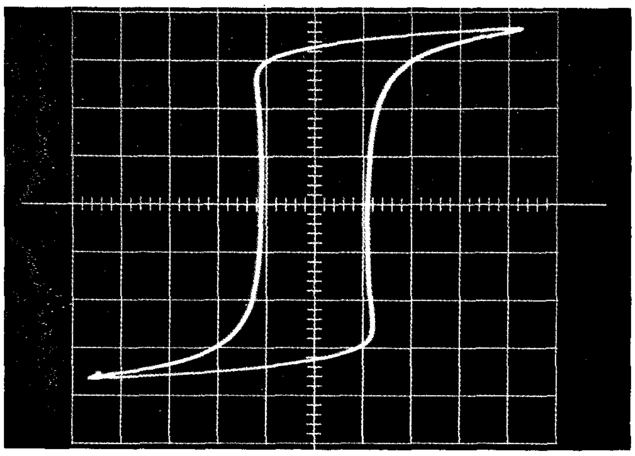

Vert = 2 KG/cm

Horiz = 10 ma/cm

Figure 13
Supermalloy F B-H Loop

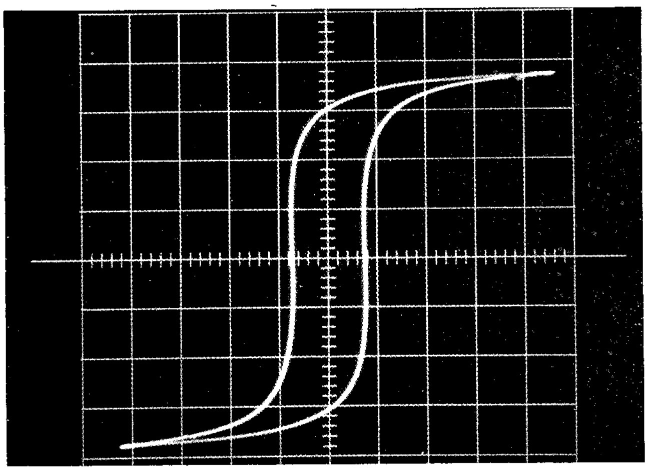

Vert = 2 KG/cm

Horiz = 10 ma/cm

Figure 14
Composite 52029-2K, A, H, D, F, B-H Loops

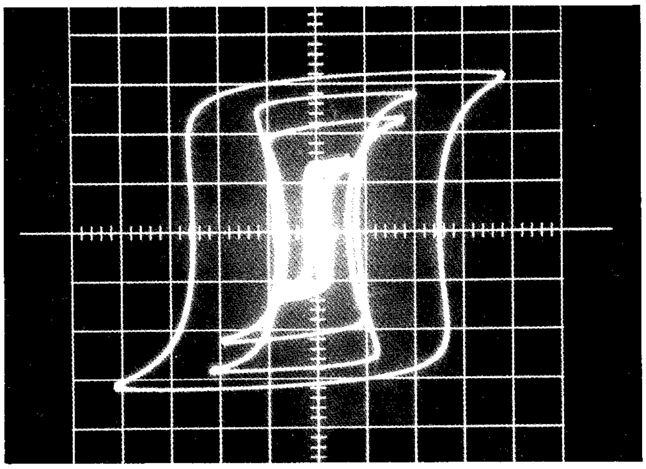

Vert = 5 KG/cm

Horiz = 50 ma/cm

Figure 15
Magnesil K B-H Loop With and Without dc

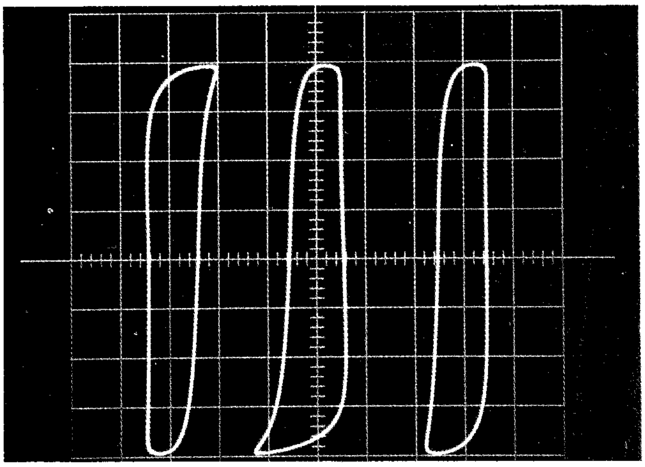

Vert = 3 KG/cm

Horiz = 200 ma/cm

Figure 16
Orthonol A B-H Loop With and Without dc

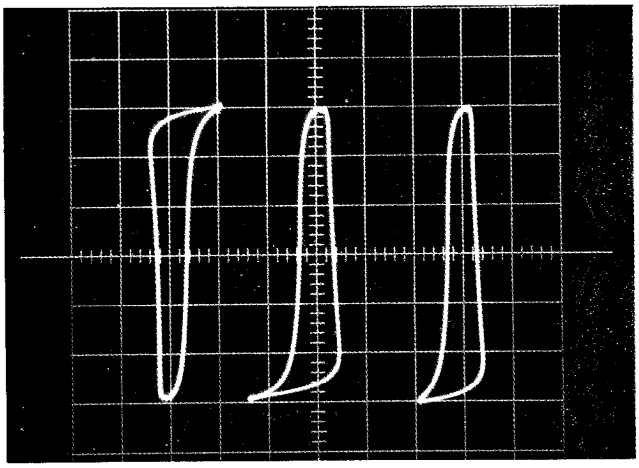

Vert = 2 KG/cm

Horiz = 100 ma/cm

Figure 17

48 Alloy H B-H Loop With and Without dc

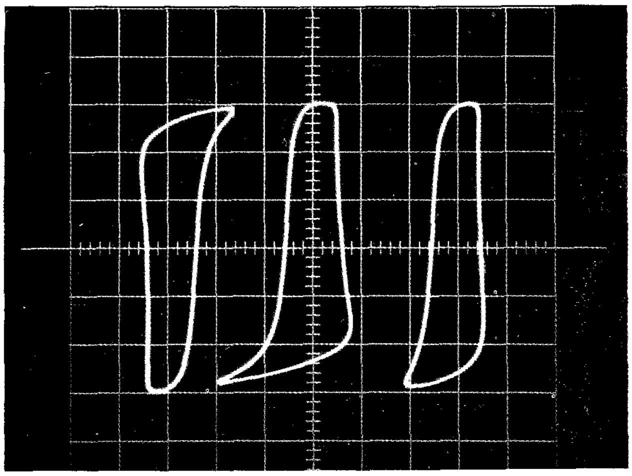

Vert = 2 KG/cm

Horiz = 50 ma/cm

Figure 18

Sq. Permalloy P B-H Loop With and Without dc

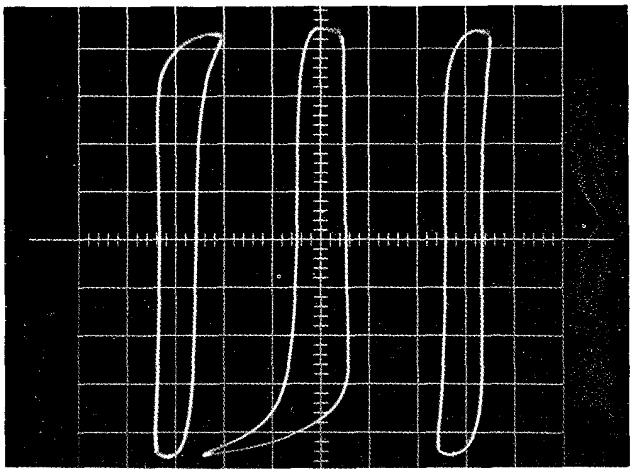

Vert = 1 KG/cm

Horiz = 20 ma/cm

Figure 19

Supermalloy F B-H Loop With and Without dc

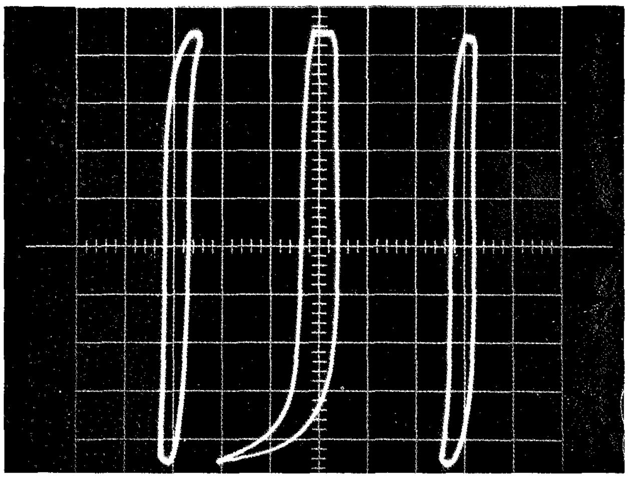

Vert = 1 KG/cm

Horiz = 20 ma/cm

Air Gap

An air gap introduced into the core has a powerful demagnetizing effect resulting in shearing over of the hysteresis loop and a considerable decrease in permeability of high-permeability materials. The dc excitation follows the same pattern. However, the core bias is considerably less affected by the introduction of a small air gap than the magnetization characteristics. The magnitude of the air gap effect also depends on the length of the mean magnetic path and on the characteristics of the uncut core. For the same air gap, the decrease in permeability will be less with a greater magnetic flux path but more pronounced in a low coercive force, high permeability core.

Effect of Gapping

Figure 20 shows a comparison of a typical toroid core B-H loop without and with a gap.

The gap increases the effective length of the magnetic path. When voltage E is impressed across primary winding N_1 of a transformer, the resulting current i_m will be small because of the highly inductive circuit shown in Figure 21.

For a particular size core, maximum inductance occurs when the air gap is minimum.

When S1 is closed, an unbalanced dc current flows in the N_2 turns, the core is subjected to a dc magnetizing force resulting in a flux density which may be expressed as:

$$B_{dc} = \frac{1.25\ N\ I_{dc}}{\ell_g + \frac{\ell_m}{\mu_{dc}}} \text{ (gauss)}$$

where

ℓ_m = Mean length (cm)
ℓ_g = Gap (cm)
B_{dc} = dc flux density (gauss)
I_{dc} = Unbalanced direct current (amperes)
μ_{dc} = dc permeability
N = Number of turns

In converter and inverter design, this is augmented by the ac flux swing which is:

$$B_{ac} = \frac{E \cdot 10^8}{K \cdot F \cdot A_c \cdot N} \text{ (gauss)}$$

where

B_{ac} = ac flux density (gauss)
E = ac voltage
F = Frequency (Hz)
A_c = Area of core (cm^2)
K = 4.0 for a square wave
K = 4.4 for a sine wave
N = Number of turns

If the sum of B_{dc} and B_{ac} shifts operation above the maximum operating flux density of the core material, the incremental permeability (μac) is reduced. This lowers

Figure 20
Air Gap Increases the Effective Length of the Magnetic Path

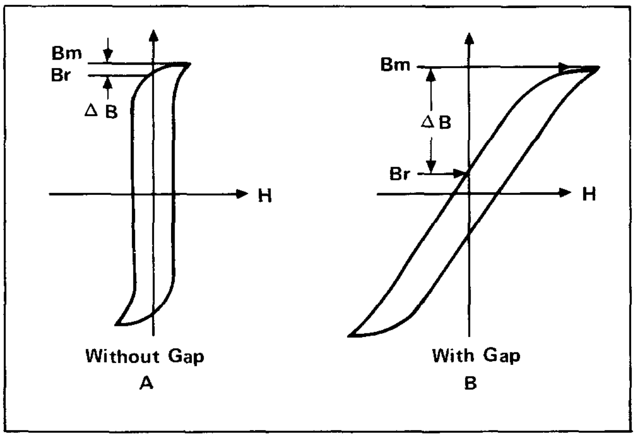

Figure 21
Implementing dc Unbalance

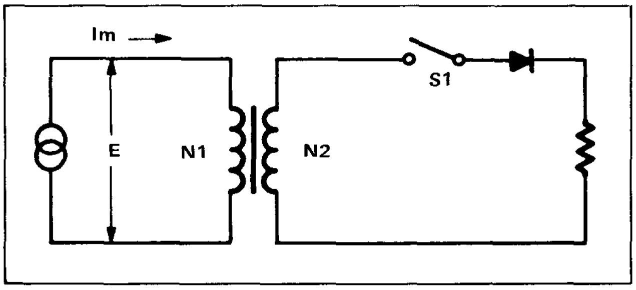

impedance and increases flow of magnetizing current i_m.This can be remedied by introducing an air gap into the core assembly which effects a decrease in dc magnetization in the core and increases ac magnetization current. However, the amount of air gap that can be incorporated has a practical limitation since the air gap lowers impedance which results in increased magnetizing current (i_m). The magnetizing current is inductive in nature. The resultant voltage spikes produced by such currents apply a great stress to the switching transistors, often causing failure. This can be minimized by tight control of lapping and etching of the gap to keep the gap to a minimum.

From Figure 20, it can be seen that the B-H curves depict maximum flux density Bm and residual flux Br for ungapped and gapped cores, and that the useful flux swing is designated ΔB, which is the difference between them. It will be noted in Figure 20A that the Br approaches the Bm, but that in Figure 20B, there is a much greater ΔB between them. In either case, when excitation voltage is removed at the peak of the excursion of the B-H loop, flux falls to the Br point. It is apparent that introducing an air gap then reduces the Br to a lower level, and increases the useful flux density. Thus insertion of an air gap in the core eliminates, or reduces markedly, the voltage spikes produced by the leakage inductance due to the transformer saturation.

Two types of core configurations were investigated in the ungapped and gapped states, namely toroidal cores and rectangular C cores. Toroidal cores as conventionally fabricated are virtually gapless. To increase the gap, the cores were physically cut in half, the cut edges lapped and acid etched to remove cut debris, and banded to form the cores. A minimum air gap on the order of less than 25 microns was established.

As will be noted from Figures 22 to 26 which are photographs showing the results of testing, the uncut and cut cores designated therein, the results obtained indicated that the effect of gapping was the same for both the C-cores and the toroidal cores subjected to testing.

It will be noted, however, that gapping of the toroidal cores produced a lowered squareness characteristic for the B-H loop as shown in table 3 (page 14); this data was tabulated from Figure 22 to 26.

Also, from Figures 22 through 26, Δ H was extracted as shown in Figure 27 and tabulated in Table 4 (page 14).

A direct comparison of cut and uncut cores was made electrically by means of two different circuit configurations. The magnetic material used in this branch of the test was Orthonol. The operating frequency was 2.4 KHz, and the flux density was 6 kilogauss (KG).

Figure 22
Magnesil 52029-2K B-H Loop Uncut and Cut

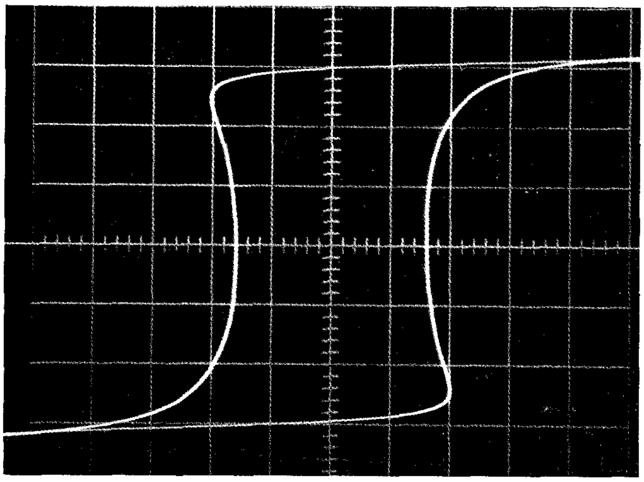

Vert = 5 KG/cm

Horiz = 100 ma/cm

UNCUT

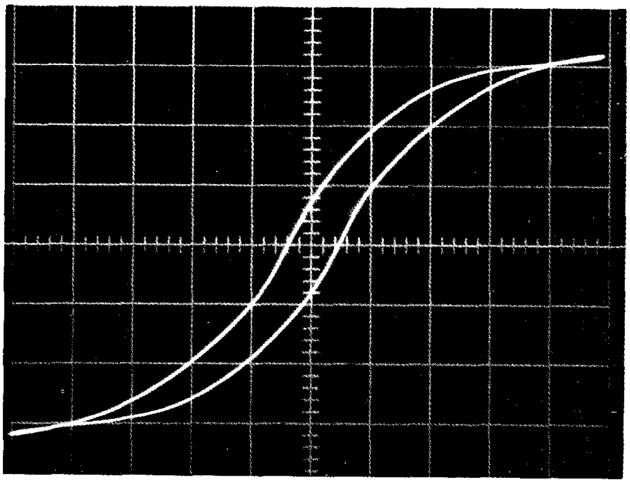

Vert = 5 KG/cm

Horiz = 500 ma/cm

CUT

Figure 23
Orthonol 52029-2A B-H Loop Uncut and Cut

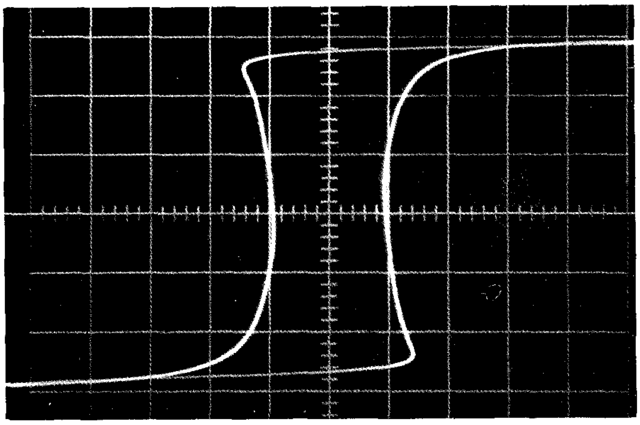

Vert = 5 KG/cm
Horiz = 50 m
UNCUT

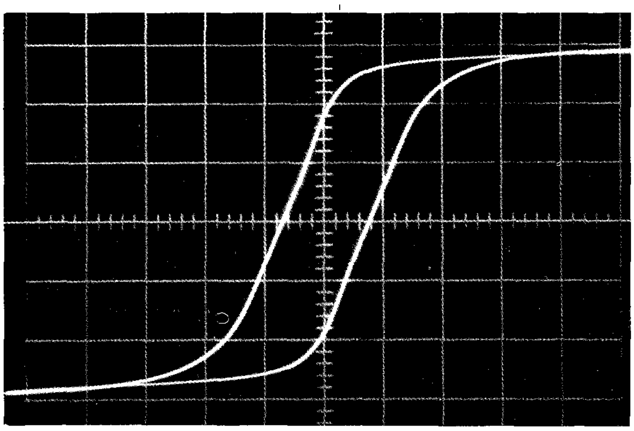

Vert = 5 KG/cm
Horiz = 100 ma/cm
CUT

Figure 24
48 Alloy 52029-2H B-H Loop Uncut and Cut

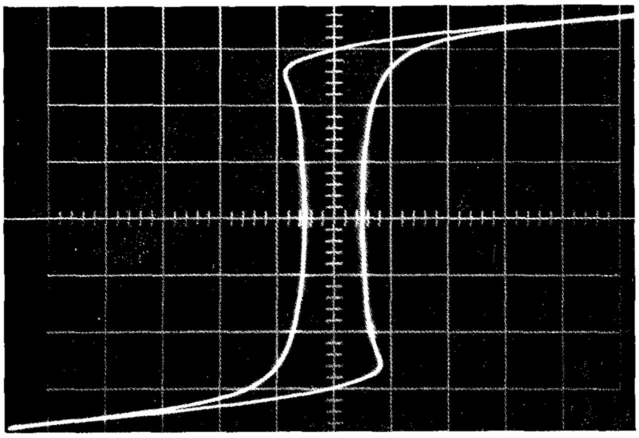

Vert = 3 KG/cm
Horiz = 100 ma/cm
UNCUT

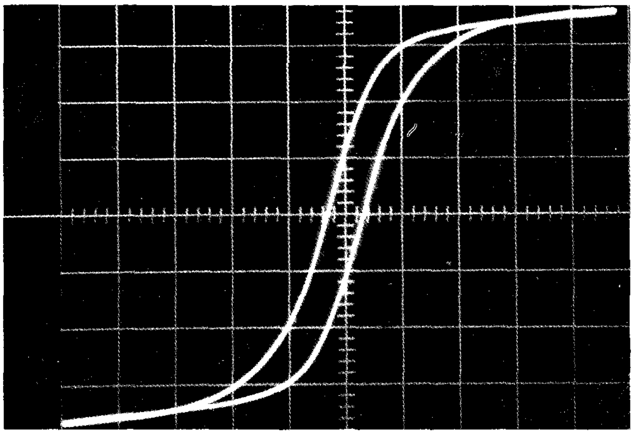

Vert = 3 KG/cm
Horiz = 200 ma/cm
CUT

Figure 25
Sq. Permalloy 52029-2D B-H Loop Uncut and Cut

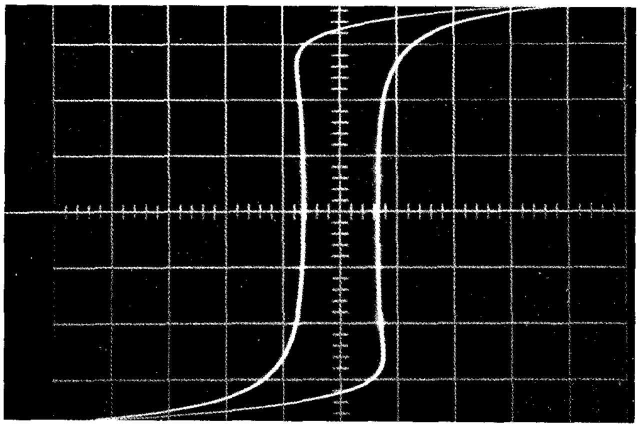

Vert = 2 KG/cm
Horiz = 20 ma/cm

UNCUT

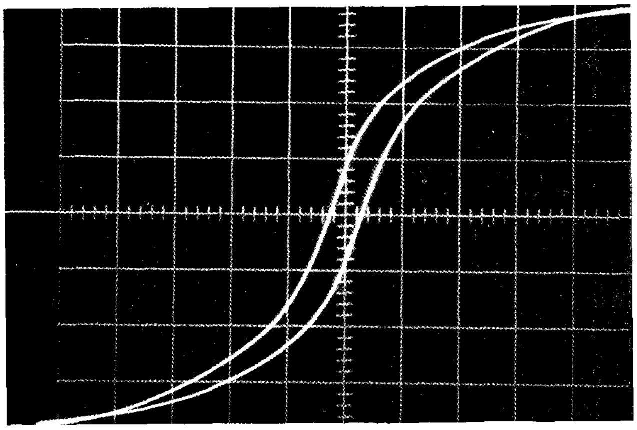

Vert = 2 KG/cm
Horiz = 100 ma/cm

CUT

Figure 26
Supermalloy 52029-2F B-H Loop

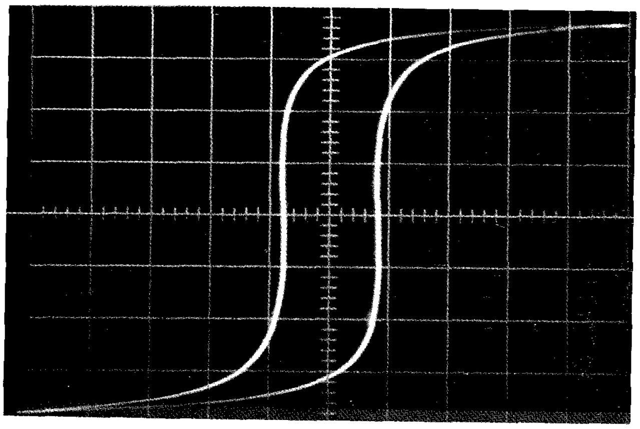

Vert = 2 KG/cm
Horiz = 10 ma/cm

UNCUT

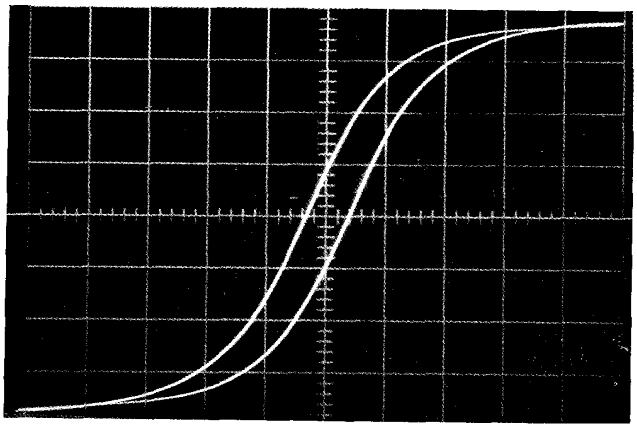

Vert = 2 KG/cm
Horiz = 50 ma/cm

CUT

Figure 28 shows a driven inverter operating into a thirty watt load, with the transistors operating into and out of saturation. Drive was applied continuously. S1 controls the supply voltage to Q1 and Q2.

With switch S1 closed, transistor Q1 was turned on and allowed to saturate. This applied E-V_C(SAT) across the transformer winding. Switch S1 was then opened. The flux in transformer T2 then dropped to the residual flux density Br. Switch S1 was closed again. This was done several times in succession in order to catch the flux additive direction. It will be noted in Figure 30 that the uncut core saturated and that inrush current was limited only by circuit resistance and transistor beta. It will also be noted in Figure 31 that saturation did not occur in the case of the cut core.

The second test circuit arrangement is shown in Figure 29. The purpose of this test was to excite a transformer, and to catch the inrush current using a current probe. A square wave power oscillator was used to excite transformer T2.

Switch S1 was opened and closed intermittently several times to catch the flux main additive direction. The photographs designated Figures 32 and 33 show inrush current for a cut and uncut core respectively.

Figure 27

Defining ΔH and ΔH_{OP}

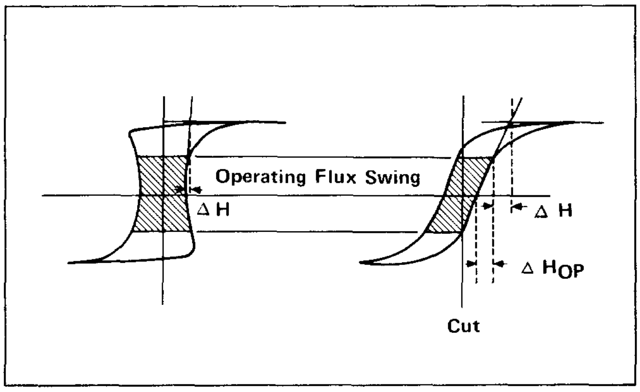

Table 3 — Comparing Br/Bm on Uncut and Cut

MATERIAL	UNCUT B_r/B_m	CUT B_r/B_m
(A) Orthonol	.96	.62
(D) Sq. Permalloy	.86	.21
(K) Magnesil	.93	.22
(F) Supermalloy	.81	.24
(H) 48 Alloy	.83	.30

Table 4 — Comparing ΔH - ΔH_{OP} on Uncut and Cut

MATERIAL	B_{MAX} KG	B_{OP} KG	B_{DC} KG	UNCUT ΔH_{OP} Oe	UNCUT ΔH Oe	CUT ΔH_{OP} Oe	CUT ΔH Oe
Orthanol	14.4	11.5	2.88	0.01	0	0.716	0.143
48 Alloy	11.2	8.9	2.24	0.02	0	1.28	0.28
Sq. Permalloy	7.3	5.8	1.46	0.008	0.004	0.787	0.143
Supermalloy	6.8	5.4	1.36	0.014	0.004	0.393	0.179
Magnesil	15.4	12.3	3.1	0.06	0.02	5.72	1.43

Figure 28
Inverter Inrush Current Measurement

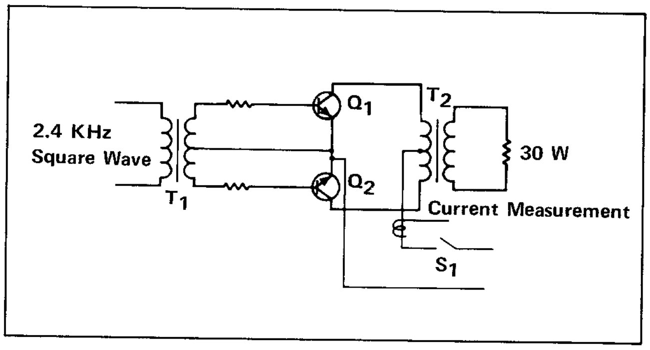

Figure 29
TR Supply Current Measurement

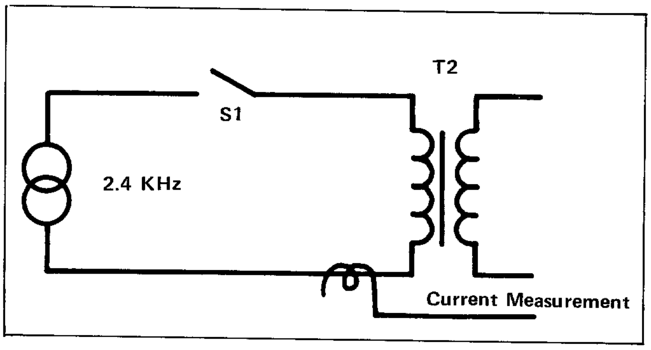

A small amount of air gap, less than 25 microns, has a powerful demagnetizing effect and this gap has little effect on core loss. This small amount of air gap decreases the residual magnetism by shearing over the hysteresis loop. This eliminates the ability of the core to remain saturated.

A typical example showing the merit of the cut-core was in the check out of a Mariner spacecraft. During the check out of a science prototype, a large (8A, 200μs) turn-on transient was observed. The normal running current is .06 amps, and is fused with a parallel redundant 1/8 amp fuse. The MM'71 design philosophy requires the use of fuses in the power lines of all "non-mission-critical" flight equipment. With this 8 amp, inrush current, the 1/8 amp fuses were easily blown. This did not happen on every turn-on, but only when the core would latch up in the wrong direction for turn-on. Upon inspection of the transformer it turned out to be a 50-50 Ni-Fe toroid. The design was changed from a toroidal core to a cut-core with a 25 micron air gap. The new design was completely successful in eliminating the 8-A turn-on transient.

Figure 30
Typical Inrush of an Uncut Core in a Driven Inverter

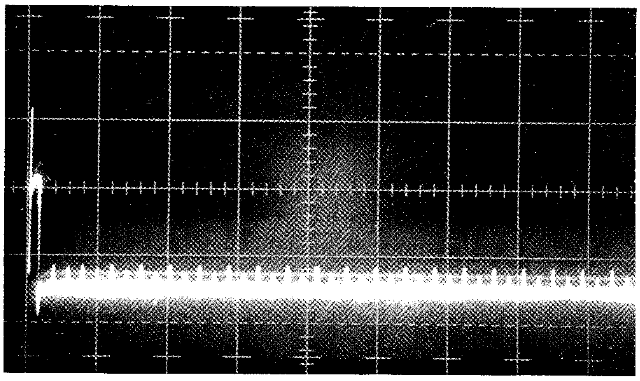

Figure 31
Same as Figure 30 But the Core was Cut and Operating With a Maximum Flux Density Value of $B_{operate} = B_{maximum} - B_{residual}$

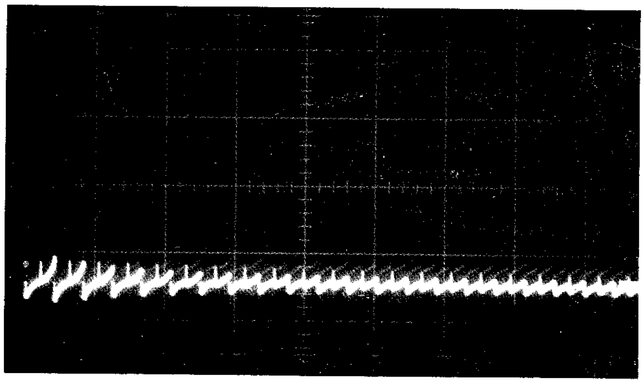

Figure 32
Typical Inrush Current of an Uncut Core Operating From an ac Source

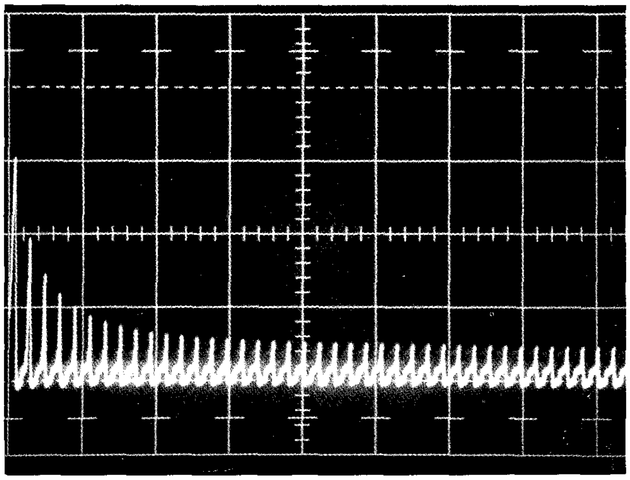

Figure 33
Same as Figure 32 But the Core was Cut and Operating With a Maximum Flux Density Value of $B_{operate} = B_{maximum} - B_{residual}$

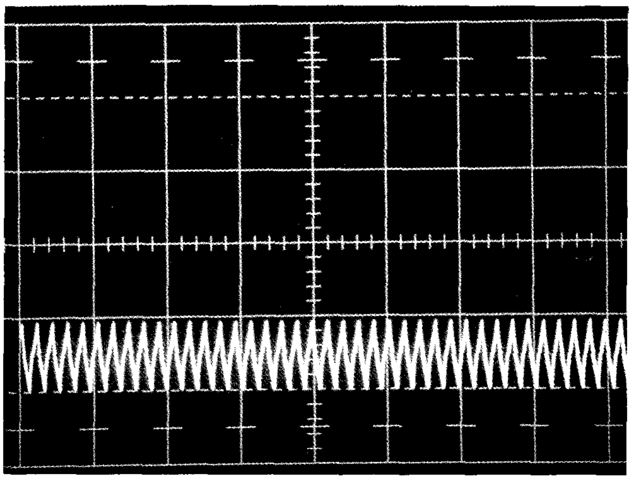

Conclusions

Low-loss tape wound toroidal core materials which have a very square hysteresis characteristic (B-H loop), have been used extensively in the design of spacecraft transformers. Due to the squareness of the B-H loops of these materials, transformers designed with them tend to saturate quite easily. The result of this is that large voltage and current spikes can occur which cause undue stress on the electronic circuitry. Saturation occurs when there is any unbalance in the ac drive to the transformer, or when any dc excitation exists. Also, due to the square characteristic, a high residual flux state (Br) may remain when excitation is removed. Reapplication of excitation in the same direction may cause deep saturation and an extremely large current spike results, limited only by source impedance and transformer winding resistance. This can produce catastrophic results.

By introducing a small (less than 25 microns) air gap into the core, the problems described above can be avoided and at the same time, the low-loss properties of the materials can be retained. The air gap has the effect of “shearing over” the B-H loop of the material such that the residual flux state is low and the margin between operating flux density and saturation flux density is high. That is to say, the air gap has a powerful demagnetizing upon the square loop materials. Properly designed transformers using “cut” toroid or “C-core” square loop materials will not saturate upon turn-on and can tolerate a certain amount of unbalanced drive or dc excitation.

It should be emphasized, however,that because of the nature of the material and the small size of the gap, extreme care and control must be taken in performing the gapping operation. Otherwise the desired shearing effect will not be achieved and the low-loss properties will be destroyed. The cores must be very carefully cut, lapped and etched to provide smooth, residue-free surfaces. Reassembly must be performed with equal care.

A Division of Spang & Company

HOME OFFICE AND FACTORY
P.O. Box 391
Butler, PA 16003
FAX: 724-282-6955
Phone: 724-282-8282
1-800-245-3984
e-mail: magnetics@spang.com
www.mag-inc.com

MPP Powder Cores • High Flux Powder Cores

KOOL MU® Powder Cores

Tape Wound Cores • Bobbin Cores

Ferrite Cores

Custom Components

Printed USA • TWC-S3 4G